Investigation of the hydrostatic pressure dependence of the E_0 gap, the excitonic binding energy and the refractive index of MOCVD-grown ZnTe layers

1992 J. Phys.: Condens. Matter 4 6401

(http://iopscience.iop.org/0953-8984/4/30/007)

J. Phys.: Condens. Matter 4 (1992) 6401–6416. Printed in the UK

Investigation of the hydrostatic pressure dependence of the E_0 gap, the excitonic binding energy and the refractive index of MOCVD-grown ZnTe layers

M Lindner, G F Schötz, P Link, H P Wagner, W Kuhn and W Gebhardt

Institut für Festkörperphysik, Universität Regensburg, W-8400 Regensburg, Universitätsstrasse 31, Federal Republic of Germany

Received 25 February 1992

Abstract. We have determined the pressure dependence of the excitonic transition energy in thin MOVPE ZnTe layers by measuring the absorption coefficient and the refractive index. Pressures up to 12 GPa were applied in a diamond anvil cell. A special gasket technique was used to suppress the scattered light. The absorption coefficient was measured in 1 μm thick films at $T = 115$ K and at $T = 300$ K up to 50 000 cm^{-1}. The spectra are dominated by a sharp excitonic structure. Its pressure dependence is evaluated using a model which allowed us to determine the rate of pressure-induced shift of the binding energy dE_x/dP and the rate of change of the Rydberg energy dR_x^*/dP. The refractive index n was measured on 2.4 μm-thick films at $T = 300$ K and at $T = 115$ K by observing the pressure shift of the interference extrema in the transparency region. The resulting refractive index was extrapolated to the frequency of the longitudinal optical phonon to obtain the constant ϵ_∞. The static dielectric constant ϵ_{st} was obtained using the Lyddane–Sachs–Teller relation. Using this value and the determined effective masses at the applied pressures, we calculated the exciton binding energy. At the pressure $P = 9.4$ GPa, a phase transition was observed. The obtained spectra for this phase were compared with a model describing indirect transitions in semiconductors. A further phase transition was observed at $P = 10.9$ GPa.

1. Introduction

The pressure dependence of the energy gaps of II–VI semiconductors has been investigated over the last 30 years [1]. The development of the diamond anvil cell [2] made measurements possible up to pressures (3–20 GPa) at which phase transitions take place [3]. The direct gaps shift sublinearly to higher energies with increasing pressure. However, if the energy of the absorption edge is plotted as a function of the relative volume change ($\Delta V/V_0$), this sublinearity mostly disappears. This behaviour was investigated theoretically by different methods like EPM [4–6] and LMTO [7] which give a very satisfactory qualitative description of the linearity. Several attempts have been made to calculate the phase transition pressures [8, 9]. These calculations also in good agreement with experimental data.

Most investigations, however, do not consider excitonic effects. Previous absorption measurements of excitons in II–VI semiconductors were made on ZnO grown by the smoke technique [10]. Other measurements were carried out on the III–V semiconductors GaAs [11] and InSe [12] by Goñi *et al.* II–VI semiconductors

0953-8984/92/306401+16$04.50

exhibit pronounced excitonic effects with an absorption coefficient near the direct gap as high as 10^5 cm^{-1}. It is difficult, therefore, to investigate the excitonic absorption in bulk materials.

If thin epitaxial films are grown by metallo-organic vapour phase epitaxy (MOVPE) [13] or by hot-wall epitaxy (HWE) [14], adequate samples of good crystal quality and with smooth surfaces become available, suitable for measurements at high absorption coefficients after the substrate has been etched off. The observation of interference patterns in the region of transparency can be used to determine the refractive index of the film.

We have investigated the pressure dependence of the excitonic absorption of free-standing ZnTe layers. A special gasket technique was employed to suppress scattered light [15]. The measured pressure dependence of the refractive index was used to obtain the values of the static dielectric constant ϵ_{st}. We derived the pressure shift of the transition energy E_x and of the Rydberg energy R_x^* on the basis of a theoretical model of excitonic absorption. A theoretical calculation of the exciton binding energy which takes into account the change of the effective masses and the change of ϵ_{st} with pressure resulted in a good agreement with the experimental data.

2. Experimental details

Transitions from the top of the valence band to the dipole-allowed 1s exciton states lead to a high absorption coefficient α ($\alpha \approx 4 \times 10^4$ cm^{-1}). As a result, very thin samples are required if we are to be able to measure the optical absorption in the excitonic region.

The samples used in this work were grown by metallo-organic chemical vapour deposition (MOCVD) on (001)-oriented GaAs substrates. The growth conditions and the investigation of the layers by photoluminescence measurements are described in [16]. The substrate was removed by chemical etching with $NaOH/H_2O_2$ solution [17]. An interferometric method was used to determine the thickness of the samples to an accuracy of 0.05% [18–20]. Optical absorption measurements were carried out in a diamond anvil cell (DAC) in combination with a nitrogen contact cryostat. A special gasket technique was developed to suppress the reflected light and the light that did not penetrate the sample. Figure 1 shows the principles of this preparation method. The inconel (72% Ni/16% Cr/8% Fe) gasket was indented in the diamond anvil cell to a thickness of 100 μm. A hole with a diameter of 100 μm was then drilled into the depression of the inconel gasket. A second hole with a diameter of 300 μm was drilled concentrically with the first hole halfway into the depression. The sample was placed on the step created by the two concentric holes. A methanol:ethanol:H_2O (80:19:1) mixture was used as the pressure-transmitting medium. The pressure was measured *in situ* using the well-developed ruby fluorescence method [21,22]. The shift of the ruby luminescence with pressure is temperature-independent [23]. At a given temperature the pressure-independent offset of the ruby luminescence has to be taken into account [24]. All pressure changes were made at room temperature to ensure good hydrostatic conditions. The sample temperature at cooling conditions was determined by comparing the zero-pressure absorption spectra in a closed DAC without the pressure medium with the temperature shift of the band edge measured by Langen *et al* [17]. For absorption measurements, white light from a tungsten lamp was focused onto the sample, forming a light spot of $\sim$ 80 μm in diameter. The

transmitted light was analysed by 66 cm Jobin–Yvon monochromator and detected by a S1 (RCA 9864QB) cathode using photon-counting equipment. Reference spectra were taken through the DAC filled with the pressure medium.

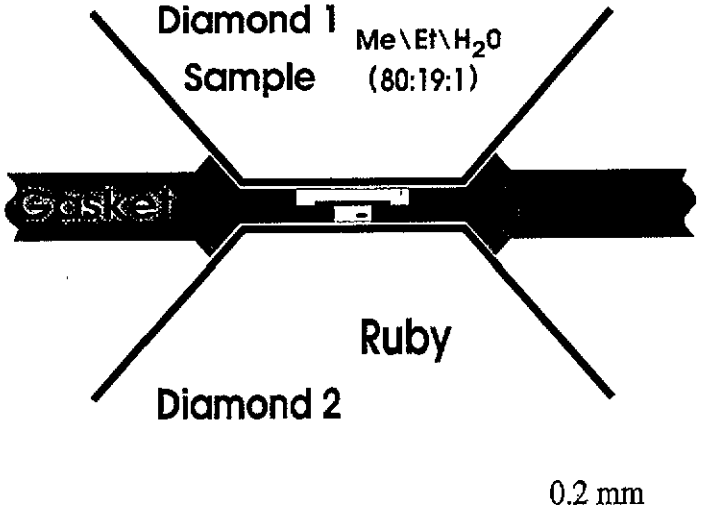

Figure 1. The gasket is simultaniously used as a pinhole. Reference spectra were taken through the gasket filled with the pressure medium.

3. Experimental results

3.1. Excitonic absorption

The pressure-dependent transmission of 1 μm-thick samples was measured at $T = 115$ K and at $T = 300$ K for pressures up to the phase transition at 9.4 GPa; in these measurements, the dark counting rate of the detector was subtracted from the transmission and from the reference spectra. A model of Swanepol describing the transmission of thin films [18] was used to obtain the absorption coefficient from the corrected transmission (the correction procedure is described below). For free-standing layers in a medium with a refractive index n', the transmission in the spectral region of strong absorbtion ($\alpha \geqslant 10^4$) is given by

$$\alpha = -\frac{1}{d} \ln \left[\frac{(n+1)^3(n+n')}{16n^2n'} \right] \frac{I_t}{I_0} \tag{1}$$

where d is the thickness of the sample, n denotes the wavelength-dependent refractive index of ZnTe, measured by Marple using the prism method [25], I_t is the light transmitted through the sample and I_0 is the given reference intensity of the lamp.

We assumed n' to equal 1.5 over the whole spectral region. The pressure dependence of the refractive index n was obtained by the method described below.

The obtained absorption coefficient was corrected using the formula

$$\frac{\alpha(P,T)}{\alpha(P=0,T=300\,\mathrm{K})} = \frac{E_0^{3/2}(P,T)}{E_0^{3/2}(P=0,T=300\,\mathrm{K})} \tag{2}$$

where P is the applied pressure and T is the sample temperature. This assumption is in agreement with the fact that the absorption strength C_0 (see equation (3)) is proportional to $E_0^{3/2}$ and the absorption coefficient α depends lineary on C_0 (for GaAs data, see [11]). Figure 2 shows typical spectra at $T = 300\,\mathrm{K}$ and at $T = 115\,\mathrm{K}$ for different pressures and compares them with curves calculated using a model described below.

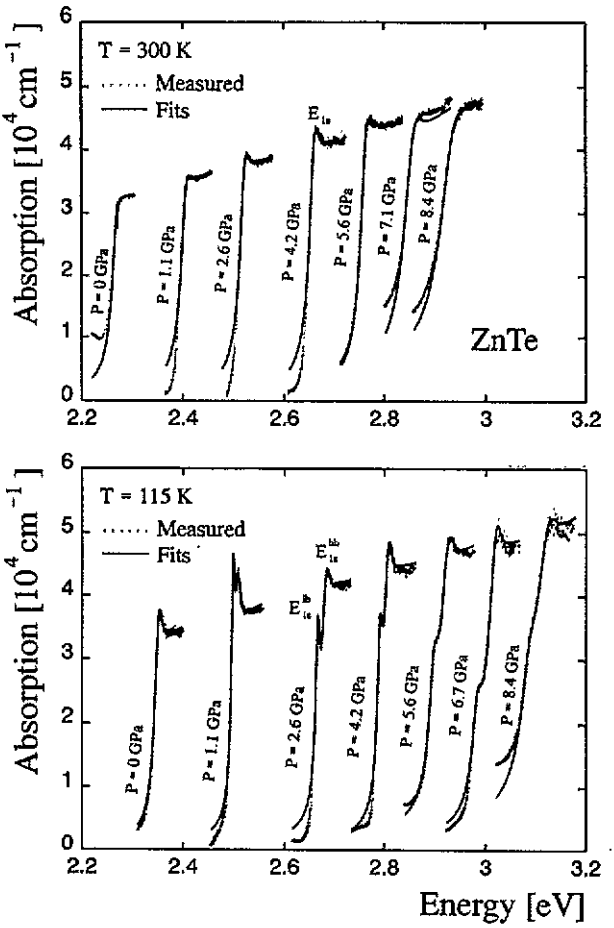

Figure 2. Pressure shift of the absorption edge of the E_0 gap at various pressures at $T = 300\,\mathrm{K}$ and $T = 115\,\mathrm{K}$ in the pressure range from 0 to 8.4 GPa.

A strong absorption peak which becomes stronger with increasing pressure was observed at $T = 300\,\mathrm{K}$; it originated from the electronic transition from the valence band to the 1s excitonic state. At $T = 115\,\mathrm{K}$, two 1s excitonic peaks were detected; this indicates the splitting of the Γ_8 valence band by a small non-hydrostatic strain

into light-hole (Γ_7) and heavy-hole (Γ_6) bands [26,27]. This strain is caused by ingrown biaxial strains of the sample and a small non-hydrostatic pressure component in the DAC.

Electronic transitions from the light-hole and the heavy-hole bands to the 1s excitonic state are dipole allowed. A theoretical evaluation of the relative intensities of the transition to the 1s excitonic states shows that the ratio $I_{hh}:I_{lh}$ is 3:1 [28].

The obtained spectra were fitted with a model describing excitonic absorption in the hydrogen-like model developed by Toyozawa [29]. Goñi [11] solved the integral for the continuous part of the absorption and obtained the expression

$$\alpha(\hbar\omega) = \frac{C_0 R_x^{*1/2}}{\hbar\omega}\left\{\sum_{m=1}^{\infty}\frac{2R_x^*}{m^3}\frac{\Gamma_m}{(\hbar\omega - E_m)^2+\Gamma_m^2} + \frac{1}{2}\left(\frac{\pi}{2} - \arctan\left(\frac{\hbar\omega + E_0}{\Gamma_c}\right)\right)\right.$$
$$\left. - \sum_{m=1}^{\infty}\frac{R_x^*}{m^3}\frac{\Gamma_c}{(\hbar\omega - E_m)^2+\Gamma_c^2} + \frac{\pi}{2}\frac{\sinh 2u^+}{\cosh 2u^+ - \cosh 2u^-}\right\} \tag{3}$$

where

$$u^{\pm} = \pi\left(\frac{R_x^{*1/2}}{2}\left(\frac{\sqrt{(\hbar\omega - E_0)^2+\Gamma_c^2} \pm (\hbar\omega - E_0)}{(\hbar\omega - E_0)^2+\Gamma_c^2}\right)\right)^{1/2}$$

$\Gamma_m = \Gamma_c - (\Gamma_c - \Gamma_1)/m^2$, $E_m = E_0 - R_x^*/m^2$, $R_x^* = \mu e^4/[2\hbar^2(4\pi\epsilon_0\epsilon_{st})^2]$, ϵ_{st} is the static dielectric constant, R_x^* is the Rydberg energy, Γ_{1s} is the half width of 1s exciton peak, Γ_c is the half width of the continuous excitonic states, $C_0 = 4\pi(2\mu)^{3/2}e^2|M_R|^2/(nc\hbar m_0^2) \sim E_0^{3/2}$ and E_{1s} is the excitonic binding energy.

The free parameters for the fit were E_{1s}, R_x^*, Γ_1 and Γ_c. C_0 is fixed by the assumption that $\alpha \sim E_0^3/2$, which differs from the use of expression (3) in [11] where C_0 is also introducted as a fit parameter. The meaning of the fit parameters is illustrated in figure 3. The summation over bound transitions runs to $n = 4$. For $T = 115$ K, a two-oscillator model was used, with $\alpha_{hh} = \frac{1}{3}\alpha_{lh}$ (see figure (3)). The most important results are given below.

The energy E_0, which describes the energy position of the excitonic continuum, increases with increasing pressure. It is usual to describe the pressure shift of the direct gap in semiconductors by the expression

$$E_0(P) = E_0(P = 0) + bP + cP^2. \tag{4}$$

In table 1 the parameters E_0, b, and c obtained by the least-squares fit are compared with those reported by other authors. The data for the pressure shift of E_0 at $T = 300$ K are in good agreement.

Figure 4 shows the pressure dependence of E_0, with the least-squares fit up to quadratic terms in pressure, and theoretical calculations based on LMTO and EPM theory. In the latter the pressure shift of the direct gap is given by

$$\frac{dE_0}{dp} = \frac{C_{12}}{a_0^2}\beta \tag{5}$$

where β denotes the compressibility, a_0 is the lattice constant, and a symmetry-dependent constant $C_{12} = 1.93 \times 10^{-18}$ eV m^2 GPa^{-1} was obtained from a least-squares fit.

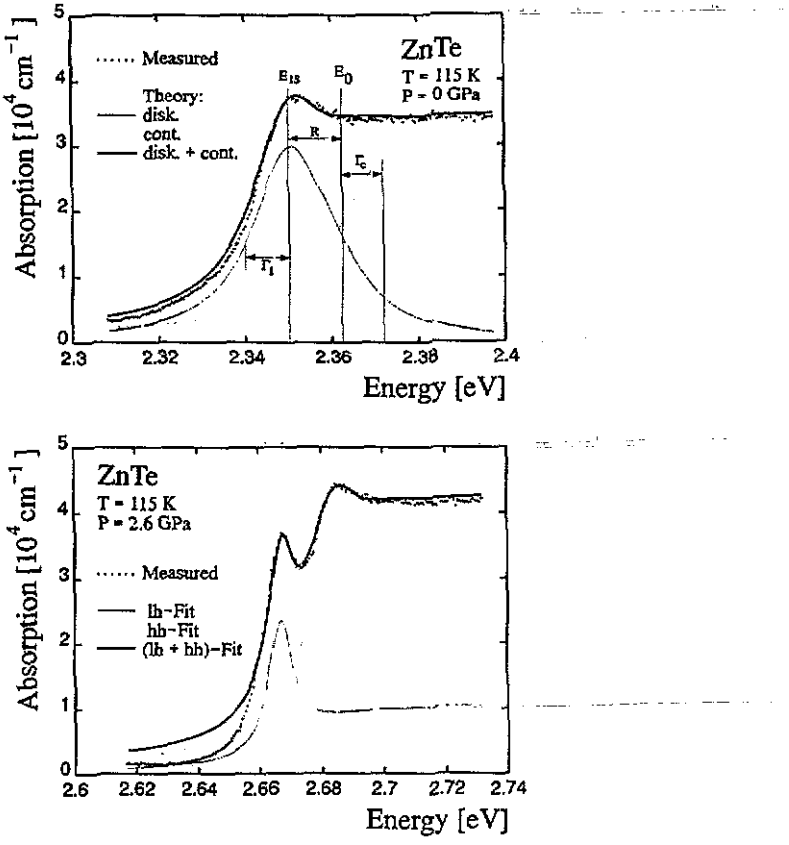

Figure 3. Examples of one-oscillator and two-oscillator fits.

Table 1. Coefficients of the least-squares fits to $E_0(P) = E_0(P=0) + bP + cP^2$ for the measured and calculated values of the pressure-induced shift in ZnTe at $T = 300$ K.

	ZnTe	E_x	b (10^{-2} eV GPa^{-1})	c (10^{-4} eV GPa^{-2})
Experiment	7.7 K[b]	2.38 ± 0.01	10.5 ± 0.5	−32 ± 5
	115 K (lh)	2.36 ± 0.01	11.3 ± 0.5	−32 ± 5
	115 K (hh)	2.36 ± 0.01	11.7 ± 0.5	−31 ± 5
	115 K [a,b]	2.36 ± 0.01	11.5 ± 0.5	−31 ± 5
	300 K[b]	2.29 ± 0.01	10.3 ± 0.5	−24 ± 5
	300 K[c]	2.27 ± 0.01	10.4 ± 0.5	−28 ± 5
	300 K[d]	2.255 ± 0.005	11.5 ± 0.5	−50 ± 3
Theory	EPM [b]	2.30	8.9	−42
	LMTO[e]	2.30	9.2	−24

[a] Mean value.
[b] Present work.
[c] Strössner *et al* [30].
[d] Weinstein *et al* [31].
[e] Christensen *et al* [7].

The resulting hydrostatic deformation potential can be obtained by plotting

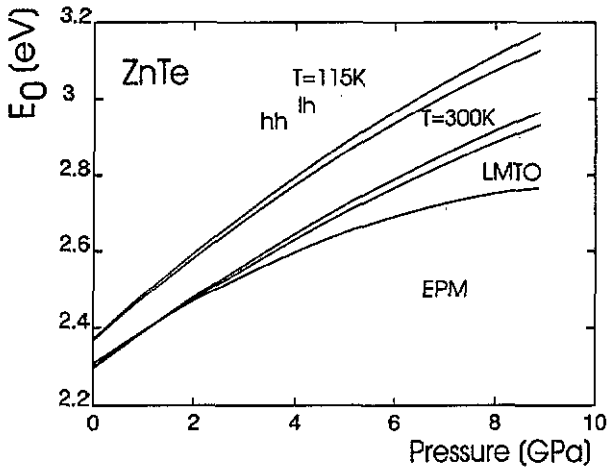

Figure 4. Pressure shift of the direct gap E_0 at $T = 300\,\mathrm{K}$ and $T = 115\,\mathrm{K}$.

Table 2. Coefficients of the least-squares fits to $E_0(a_0(P)) - E_0(a_0(P=0)) = b'P(-\Delta a_0/a_0(P=0)) + c'(-\Delta a_0/a_0(P=0))^2$ for the measured and calculated values of the pressure shift in ZnTe at $T = 300\,\mathrm{K}$

ZnTe	b' (eV)	c' (eV)
Experiment	15.8 ± 0.1[a]	-2.92 ± 3[a]
	16.2 ± 0.1[b]	0 ± 3
Theory	15.5[a]	−105[a]
	19.1[b]	−164[b]
	13.8[c]	18.0[c]

[a] Present work (EPM).
[b] Strössner *et al* [30] (EPM).
[c] Christensen *et al* [7] (LMTO).

the pressure shift of E_0 versus volume at the applied pressure. The hydrostatic deformation potential is given by

$$a_{dp} = \frac{\partial E_0}{\partial(\ln V)} \approx \frac{\Delta E_0}{\Delta V(P)/V_0}. \tag{6}$$

The volume change was obtained using Murgnahan's equation of state [33]

$$V(P) = \frac{V_0}{(1 + (B'/B_0)P)^{1/B'}} \tag{7}$$

and the dependence on the hydrostatic pressure of the lattice constant was taken to be that measured by x-ray diffraction at $T = 300\,\mathrm{K}$ by Strössner *et al* [30]. For the bulk modulus, they obtained $B_0 = 48.0\,\mathrm{GPa}$ and for its pressure derivative, $B' = 4.7$. In figure 5, the change of the energy E_0 is plotted versus the relative change of the lattice constant, $\Delta a_0/a_0(P=0)$. The curves obtained were described by the relation

$$E_0(a_0(P)) - E_0(a_0(P=0)) = b'\left(-\frac{\Delta a_0}{a_0(P=0)}\right) + c'\left(-\frac{\Delta a_0}{a_0(P=0)}\right)^2. \tag{8}$$

The energy gap increases linearly with the change of the lattice constant. The coefficients b' and c' are given in table 2.

The deformation potential thus derived is

$$a_{dp} = -5.3 \pm 0.2 \text{ eV} \qquad \text{for } T = 300 \text{ K}.$$

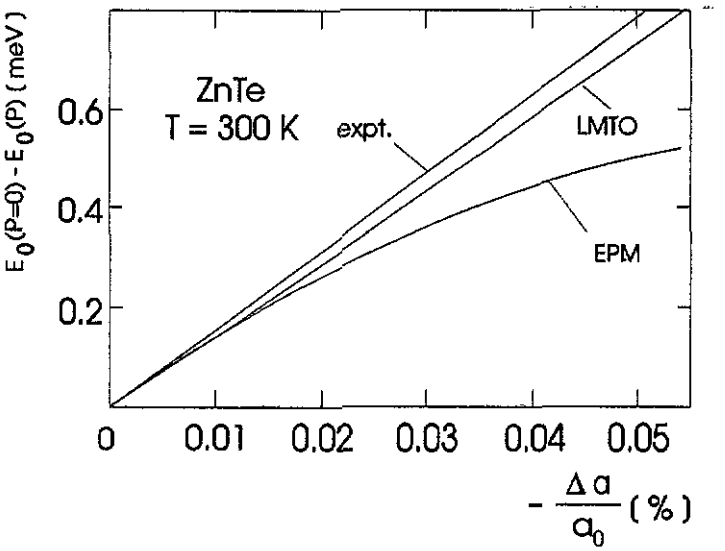

Figure 5. The exciton binding energy as a function of the relative volume change $\Delta a/a_0$. The hydrostatic deformation potential a_{dp} is obtained from the slope of the straight line.

The exciton binding energy obtained increases with pressure. A similar behaviour was observed by Goñi *et al* on GaAs [11] and was explained qualitatively by an increase in the effective masses with increasing pressure. In figure 6 the enhancement of the exciton binding energy with increasing pressure is shown for $T = 115$ K and for $T = 300$ K, together with a theoretical evaluation which is described later in this paper. The experimentally found increase in the Rydberg energy dR_x^*/dp is 10 meV GPa^{-1}.

A broadening of the half-width Γ_{1s} of the excitonic peak appears at $P = 5$ GPa for $T = 300$ K and at 3.3 GPa for $T = 115$ K. The same effect is apparent in the measurements of Weinstein *et al* [31] and Strössner *et al* [30], where the slope of the absorption decreases at $P \approx 6$ GPa. This behaviour may be due to the generation of point defects, which result in additional scattering processes and thus cause a decrease in the lifetime of the excitonic states. Indirect transitions can be excluded in the zincblende phase, by using estimates of the $E_L \rightarrow E_\Gamma$ and the $E_\Gamma \rightarrow E_X$ pressure shifts [34].

3.2. Pressure dependence of the refractive index

Interference patterns were observed on samples with smooth surfaces. The refractive index was obtained at wavelengths of interference maxima and minima in the region of transparency ($\alpha = 0$) using the formula for normal incidence,

$$2n(\lambda, P)d = m\lambda \tag{9}$$

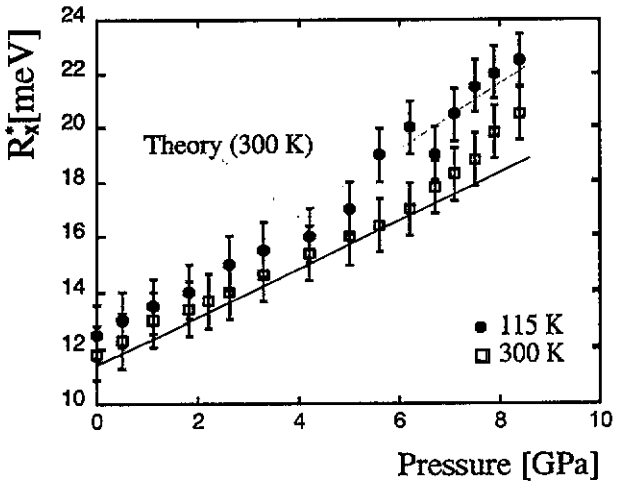

Figure 6. Exciton binding energy R_x^* as a function of pressure (see text), together with a theoretical evaluation (see section 4).

where m is the order of the interference extrema. This relation was used to determine the pressure dependence of the refractive index. Crystal slabs prepared for these measurements had a typical thickness of 2.4 μm. After measuring the interference patterns up to 7 GPa, the pressure was slowly lowered to zero pressure, to make sure that the same spot of the sample was examined at all pressures. One interference maximum was observed by slowly increasing the pressure throughout the measurement. Figure 7 shows some of the spectra obtained at $T = 300$ K. At $T = 115$ K the same procedure was used to obtain the refractive index; but now the temperature dependence of thickness had to be taken into account, using the thermal expansion coefficient measured by Novikova and Abrikosov [35]. The deviation from continuous growth of transmission at high pressures in the low-energy spectral region is due to interference between the DAC and the sample, which we were unable to suppress even though we adjusted the DAC carefully. From the zero-pressure spectrum, the exact thickness was evaluated to an accuracy of 0.05% via formula (9), using the wavelength-dependent refractive index measured by Marple [25]. The orders of the interference maxima and minima were determined by a method developed by Swanepol [18]. The refractive index at the energy positions of the interference extrema at the pressures measured can then be obtained again using formula (9) and taking into account the decrease of thickness with increasing pressure.

Figure 8 shows the refractive index for several values of pressure at $T = 300$ K and $T = 115$ K, in the spectral region from E_x to 900 nm, together with the refractive index obtained by Marple. The accuracy obtained by this method is within 0.3%.

For the pressures applied, the measured refractive index was fitted to Marple's formula for the wavelength dependence of the refractive index [25]

$$n(\lambda) = A(P) + \frac{B(P)\lambda^2}{\lambda^2 - C(P)} \tag{10}$$

using three semiempirical parameters $A(P)$, $B(P)$ and $C(P)$. A is a constant background dielectric constant, B is a measure of the oscillator strength near the E_0

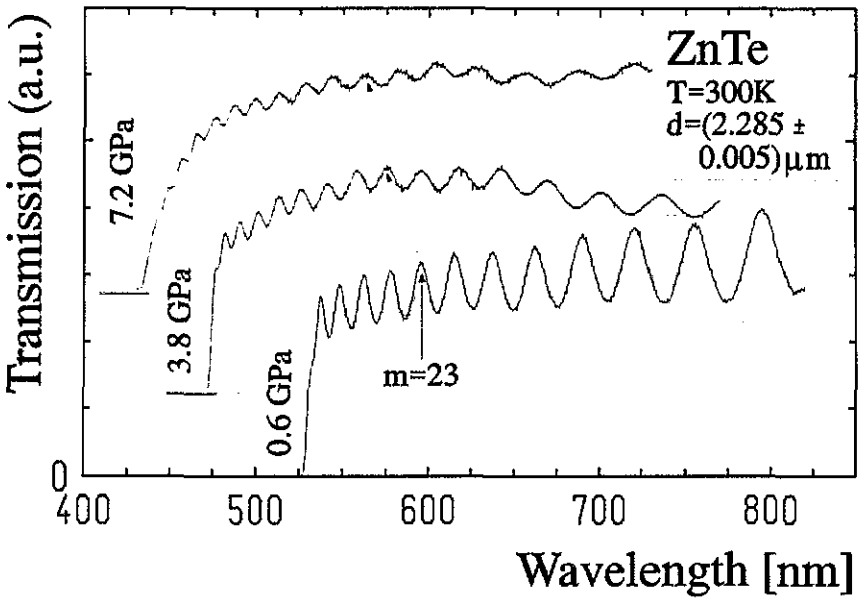

Figure 7. Interference fringes recorded in the transparency range of a ~ 2.285 μm-thick layer.

gap, while C is a characteristic wavelength for these transitions. The wavelength λ in this formula is given in μm. The parameters A, B and C were obtained by a least-squares fit to the experimental data at the applied pressure P.

In figure 9, A, B and C are plotted versus pressure. The pressure dependence of the fit parameters was described using the function

$$X(P) = X_0(P) + X_1P + X_2P^2 \tag{11}$$

with $X = A$, B and C. The parameters X_0, X_1 and X_2 obtained are summarized in table 3. The linear decrease of A is due to the shifting of higher gaps with pressure, which causes a decrease in the background dielectric constant in the visible range. The increase in B is due to the increase in the oscillator strength with pressure, while the decrease in C can be explained by the pressure shift of the E_0 gap to higher energies.

Table 3. Pressure dependence of the fit parameters X_0, X_1 and X_2 obtained by a least-squares fit.

X	X_0	X_1	X_2	T
A	5.8 ± 0.1	-0.15 ± 0.2	0	300 K
	5.5 ± 0.1	-0.19 ± 0.2	0	115 K
B	1.8 ± 0.1	-0.14 ± 0.2	0	300 K
	1.9 ± 0.1	-0.18 ± 0.2	0	115 K
C	0.182 ± 0.003	$(-1.8 \pm 0.05) \times 10^{-2}$	$(-1.08 \pm 0.05) \times 10^{-3}$	300K
	0.166 ± 0.003	$(-1.7 \pm 0.05) \times 10^{-2}$	$(-1.09 \pm 0.05) \times 10^{-3}$	115 K

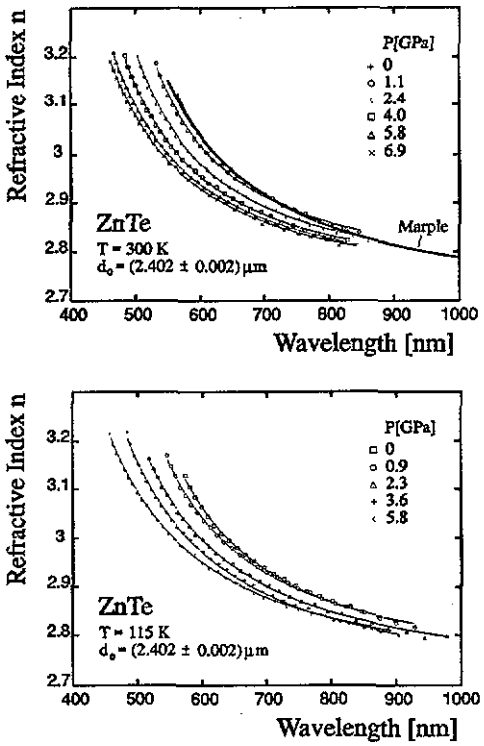

Figure 8. Pressure dependence of the refractive index of ZnTe in the spectral range from E_x to 900 nm at $T = 300$ K and $T = 115$ K, together with the refractive index data reported by Marple.

3.3. Phase transitions

A change in crystal structure was observed by Strössner *et al* [30] at $P = 9.4$ GPa and by Ohno *et al* at 8.7 GPa [32]. These authors also observed a drastic change in conductivity and showed by x-ray diffraction that the phase transition takes place between zincblende and rocksalt structures.

At $P = 9.4$ GPa our samples show a change in colour from light yellow to red. Absorption spectra were made at pressures between 9.4 and 10.9 GPa at $T = 300$ K. The spectra show no change in this pressure region. The spectrum at 9.4 GPa is shown in figure 10. In the low-energy region the absorption coefficient increases again. This behaviour was explained as being due to free electrons created by lattice defects in the high-pressure phase. In figure 10 the square root of the absorption coefficient $\sqrt{\alpha}$ is plotted as a function of energy for the high-energy part of the spectrum. It shows a linear behaviour. This is typical of semiconductors with an indirect gap. An evaluation of the indirect gap was obtained by extrapolating to $\alpha = 0$. It was found to lie at 0.6 eV.

Similar spectra were obtained for other II–VI compounds in the rocksalt phase. This happens to be the case for CdO [36] at room temperature and normal pressure, and for the high-pressure phases of CdS [37] and ZnS [38]. The absorption of CdO and CdS in the rocksalt structure was interpreted to be indirect, with gap energies of 1.3 eV and 1.5 eV, respectively. The indirect gap of ZnS was found near 2 eV.

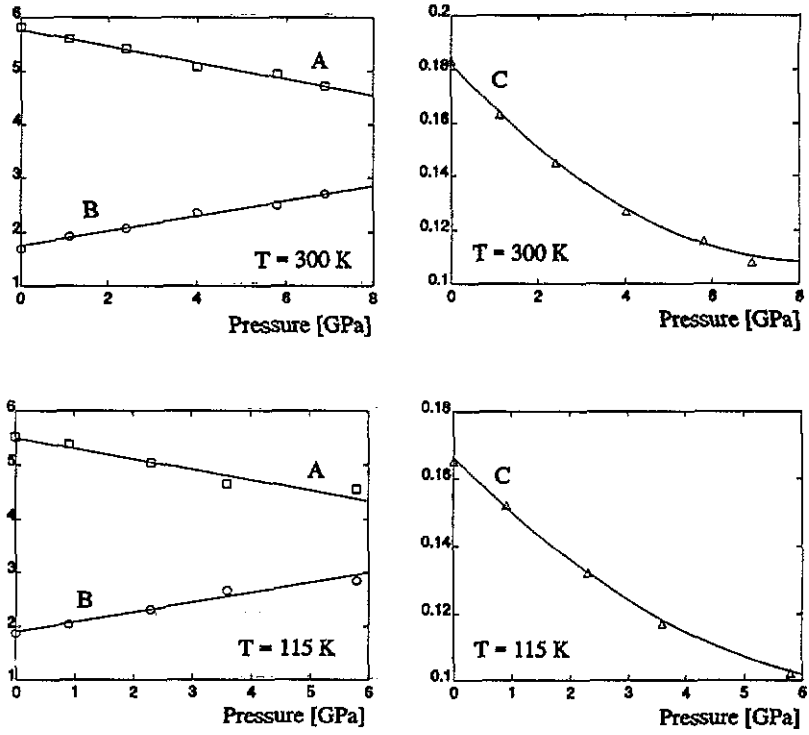

Figure 9. Pressure dependence of the fit parameters A, B and C at $T = 300\,\mathrm{K}$ and $T = 115\,\mathrm{K}$.

Maschke and Rössler [39] determined the band structure of CdO (RS) and obtained an indirect gap with an energy of ~ 1 eV. The conduction-band minimum lies between the X and the K points in the Brillouin zone. Similar calculations were carried out by Liu and Rabii [40] for the rocksalt phase of CdS ($P \geqslant 2.3\,\mathrm{GPa}$) and indicated an indirect-gap energy of 1.5 eV. At $P = 10.9\,\mathrm{GPa}$, a phase transition to a metallic state was observed.

4. Theoretical determination of the exciton binding energy

We calculate the pressure dependence of the Rydberg energy of the exciton using the well-known relation

$$R_x^*(P) = R_\mathrm{H}\frac{\mu(P)}{\epsilon_{st}(P)} \tag{12}$$

where $R_\mathrm{H} = m_0 e^4/(2\hbar^2(4\pi\epsilon_0\epsilon_{st})^2)$ is the Rydberg energy of the hydrogen atom, $\mu = m_c(P) + m_h(P)/(m_c(P)m_h(P))$ is the reduced mass of the exciton and $\epsilon_{st}(P)$ is the static dielectric constant at a pressure P.

The effective electron mass in the conduction band and that of the light hole and the heavy hole in the valence band at arbitary pressure can be calculated using the $k\cdot p$ theory [26,42]. Kane [41] developed a model for effective masses as functions of gap energy for semiconductors of zincblende structure, taking into account exactly the

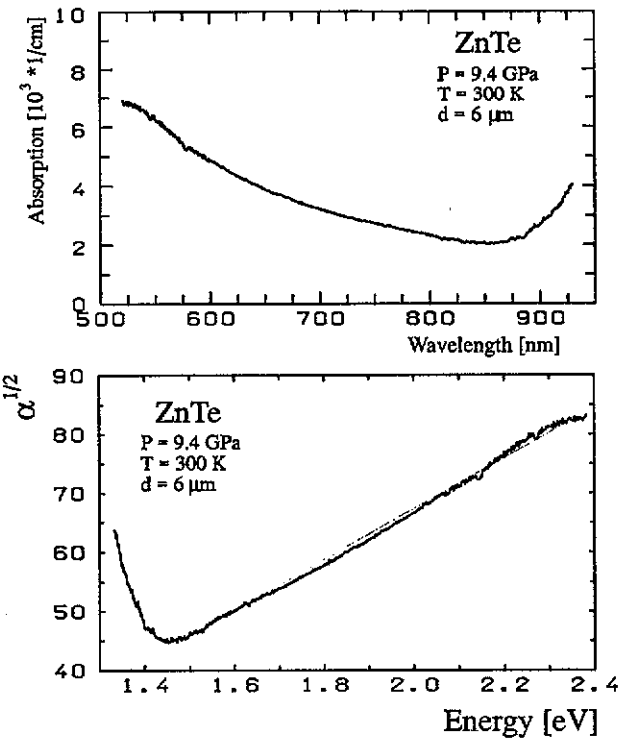

Figure 10. Absorption spectrum of the ZnTe high-pressure phase and E as a function of $\sqrt{\alpha}$.

k-independent spin–orbital interaction and the effect of higher bands by second-order perturbation theory using an 8×8 perturbation matrix. The 8×8 matrix splits into two identical 4×4 matrices with the energies

$$E_{cb}(k) = E_0 + \frac{\hbar^2 k^2}{2m} + \frac{M^2 k^2}{3}\left(\frac{2}{E_0} + \frac{1}{E_0 + \Delta}\right) \tag{13}$$

for the conduction band,

$$E_{hh}(k) = \frac{\hbar^2 k^2}{2m} \tag{14}$$

for the heavy-hole band and

$$E_{lh}(k) = \frac{\hbar^2 k^2}{2m} - \frac{2M^2 k^2}{3E_0} \tag{15}$$

for the light-hole band.

The dispersion relation for the split-off band is given by

$$E_{so}(k) = -\Delta + \frac{\hbar^2 k^2}{2m} - \frac{2M^2 k^2}{3(E_0 + \Delta)}. \tag{16}$$

Here Δ is the spin–orbital splitting between the degenerate valence band ($J = 3/2$) and the split-off valence band ($J = 1/2$), and the real quantity M is defined as $(-i\hbar/m)(S|p_z|Z)$. The effective masses were obtained by the well-known relation $1/m^* = d^2E(k)/dk^2$. Introducing the quantity $T^2 = m_0\hbar^2M^2$ and assuming Δ to be pressure independent, we obtain for the effective mass of the electron in the conduction band the expression

$$\frac{m_0(P)}{m_c(P)} = 1 + 2T^2\frac{E_0(P) + \frac{2}{3}\Delta}{E_0(P)(E_0(P) + \Delta)}. \tag{17}$$

The above assumption is based on the experiments of Brothers and Brunghardt [43], who measured the pressure dependence of some higher gaps in ZnTe, and found a pressure-independent value for the spin–orbit splitting: $\Delta = 0.96$ eV.

The effective mass of the light hole at the valence band edge is

$$\frac{m_0}{m_{lh}} = -\left[1 - \frac{4T^2}{3E_0(P)}\right]. \tag{18}$$

The effective mass m_{hh} of the heavy hole at the valence band edge is constant in this appoximation. It is well known that the Kane model does not describe the dispersion of the heavy hole very well. Therefore, we express m_{hh} by the Luttinger parameters calculated from [44]. Perturbations by remote-band interaction were not taken into account.

With these values of the effective mass, we obtain the matrix element of momentum $T^2 = 9.5 \pm 0.1$ eV, which is in good agreement with the value of 9.4 eV obtained by Cardona [45].

To determine the effective mass of the valence band, we chose the approximation

$$\frac{1}{m_{vb}} = \frac{1}{2}\left(\frac{1}{m_{lh}} + \frac{1}{m_{hh}}\right).$$

The pressure dependence of the effective masses was calculated using relations (17) and (18) and the measured shift of E_x as a function of pressure. The static dielectric constant ϵ_{st} was obtained by extrapolating the refractive index n to the longitudinal optical frequency ω_{LO}, with a phenomenological fit for the refractive index by the parameters A, B and C as described in section 3.2. In this way we obtained the high-frequency dielectric constant $\epsilon_\infty = n^2 = 7.4 \pm 0.2$. This value was found to be pressure-independent within the accuracy of the measurement.

From ϵ_∞ we calculated ϵ_{st} using the Lyddane–Sachs–Teller relation

$$\frac{\epsilon_{st}}{\epsilon_\infty} = \frac{\omega_{LO}^2}{\omega_{TO}^2} \tag{19}$$

where ω_{LO} and ω_{TO} are the pressure-dependent frequencies of the LO and TO phonons, respectively. These frequencies were measured by Weinstein [46] using the room-temperature Raman scattering and the static dielectric constant $\epsilon_{st}(P = 0) = 9.8 \pm 0.2$. The pressure dependence of ϵ_{st} can be described by the expression

$$\epsilon_{st}(P) = 9.8 - 0.281P + 0.0076P^2. \tag{20}$$

In figure 6, the theoretical pressure shift of the Rydberg energy (0.75 meV GPa^{-1}) is compared with the experimental observations. One can see that the values agree within 10%. The discrepancies may be caused by neglect of the exchange interactions and polaronic effects in the theoretical and experimental analysis.

5. Summary

This paper presents measurements of the pressure-dependent excitonic absorption at the direct gap E_0 and of the refractive index n of ZnTe MOCVD-grown films on (100)-oriented GaAs substrates. Free-standing layers were obtained by selective etching of the substrate with $NaOH/H_2O_2$ solution. The measurements were carried out in a diamond anvil cell at $T = 115$ K and at $T = 300$ K up to the phase transition at 9.4 GPa. A special gasket technique was used to suppress scattered light. The 1s exciton peak was accurately recorded in 1 μm-thick samples. At $T = 115$ K, two 1s peaks were observed, reflecting the splitting of the valence band by a small ingrown biaxial strain depending on growth conditions, lattice defects and non-hydrostatic components in the DAC. The absorption coefficient was obtained using a model describing transmission through thin films. The spectra were fitted with Toyozawa's model of the excitonic absorption in the hydrogen-atom approximation, and the pressure dependence of E_0 and R_x^* were obtained. The obtained dE_0/dP is in good agreement with the results for bulk crystals; the mean value for dR_x^*/dP is 0.8 meV GPa^{-1}. This change was compared with a theoretical calculation, which takes into account the change in the effective masses of m_c, m_{lh} and m_{hh} and the change in the static dielectric constant with pressure. $\epsilon_{st}(P)$ was obtained by determining the refractive index n in the transparency band. The refractive index n was calculated from the wavelength shift of the interference patterns, and n^2 was extrapolated to ω_{LO}. We thus obtained a pressure-independent value for $\epsilon_\infty = n_\infty^2 = 7.4 \pm 0.2$. The value of ϵ_{st} was calculated using the Lyddane–Sachs–Teller relation. The calculated values of $R_x^*(P)$ agree within 10% with the results of the measurements.

Absorption spectra in the high-pressure phase at 300 K exhibit a shape typical of an indirect transition, with a gap at 0.6 eV. No pressure-induced shift of absorption was observed. Theoretical calculations show that the smallest gap in RS-structure semiconductors lies between the X and the K points. The calculated gap width is ≈ 1 eV. An increase in the absorption coefficient in the low-energy range is explained by free electrons created by lattice defects in the high-pressure phase.

Acknowledgments

We would like to thank J Ploner for technical assistance and S Luber, X Wolf and P Müller for preparing the samples. This work was supported by Deutsche Forschungsgemeinschaft (DFG).

References

[1] Camphausen D L, Connell G A N and Paul W 1971 *Phys. Rev. Lett.* **26** 184
[2] Barnett J D, Block S and Piermani G J 1973 *Rev. Sci. Instrum.* **4** 1
[3] Yu S C, Spain I L and Skelton E F 1978 *Solid State Commun.* **25** 49
[4] Sandrock R 1970 *Festkörperprobleme* p 283
[5] Melz P J 1967 *J. Phys. Chem. Solids* **28** 1441
[6] Cohen M L 1982 *Phys. Scr.* T **1** 5
[7] Christensen N E and Christensen O B 1986 *Phys. Rev.* B **33** 4739
[8] Soma T 1978 *J. Phys. C: Solid State Phys.* **11** 2681
[9] Singh R K and Singh S 1989 *Phase Transitions* **15** 127
[10] Huffman D R, Schwalbe L A and Schiferl D 1982 *Solid State Commun.* **44** 521

[11] Goñi A, Cantarero A, Syassen K and Cardona M 1990 *Phys. Rev.* B **41** 10111
[12] Goñi A, Schwarz U, Cantarero A, Syassen K and Segura A 1990 *Bull. Am. Phys. Soc.* **35** 618
[13] 1990 *Advanced Materials* vols 8, 9 p 282
[14] Link P 1992 *Thesis* Universität Regensburg
[15] Lindner M, Wagner H P, Kuhn W and Gebhardt W High Pressure Research 1991 *Proc. XXVIIIth EHPRG (Bordeaux, 1990)* p 412
[16] Wagner H P, Kuhn W and Gebhardt W 1990 *J. Cryst. Growth* **101** 199
[17] Langen B, Leiderer H, Limmer W and Gebhardt W 1990 *J. Cryst. Growth* **101** 718
[18] Swanepol R 1983 *J. Phys. E: Sci. Instrum.* **16** 1214
[19] Swanepol R 1984 *J. Phys. E: Sci. Instrum.* **17** 897
[20] Bishop M F 1976 *Solid State Commun.* **20** 779
[21] Adams D M, Appleby R and Shang S K 1976 *J. Phys. E: Sci. Instrum.* **9** 1140
[22] Forman R A, Piermani G J and Block D S 1972 *Science* **176** 284
[23] Noack R A and Holzapfel W B *High Pressure Science and Technology* ed K D Timmerhaus and M S Barber, vol 11 (New York :Plenum) p 748
[24] Vos W L and Schouten J A 1991 *J. Appl. Phys.* **69** 6744
[25] Marple D T F 1964 *J. Appl. Phys.* **35** 539
[26] Pikus G E and Bir G L 1959 *Fiz. Tverd. Tela* **11** 1642 (Engl. Transl. 1959 *Sov. Phys.–Solid State* **1** 1502)
[27] Leiderer H, Supritz A, Silberbauer M, Lindner M, Kuhn W, H P Wagner and Gebhardt W 1991 *Semicond. Sci. Technol.* A **6** 101
[28] Pollack F H and Cardona M 1968 *Phys. Rev.* **72** 816
[29] Toyozawa Y 1958 *Prog. Theor. Phys.* **20** 53
[30] Strössner K, Ves S, Chui Koo Kim and Cardona M 1986 *Solid State Commun.* **61** 275
[31] Weinstein B A, Zallen R and Slade M L 1981 *Phys. Rev.* **24** No 8
[32] Ohno Y, Endo S, Kobayashi M and Narita S 1983 *Phys. Lett.* **95A** 407
[33] Murgnahan F D 1944 *Proc. Natl Acad. Sci.* **30** 244
[34] Harrison W A 1973 *Phys. Rev.* B **8** 4487
[35] Novikova S I and Abrikosov N K 1963 *Sov. Phys.–Solid State* **5** 1558
[36] Kocka J and Konak C 1971 *Phys. Status Solidi* b **43** 731
[37] Batlogg B, Jayaraman A, Van Cleve J E and Maines R G 1983 *Phys. Rev.* B **27** 3920
[38] Ves S, Schwarz U, Christensen N E, Syassen K and Cardona M 1991 *Phys. Rev.* B **42** 9113
[39] Maschke K and U Rössler 1968 *Phys. Status Solidi* b **28** 577
[40] Liu W W and Rabii S 1976 *Phys. Rev.* B **13** 1675
[41] Kane E O 1957 *J. Phys. Chem. Solids* **1** 249
[42] Drouhin H J and Peretti J 1991 *Phys. Rev.* B **44** 7993
[43] Brothers A D and Brunghardt J B 1980 *Phys. Status Solidi* b **99** 291
[44] Wagner H P *et al* 1976 *J. Lumin.* to be published
[45] Cardona M 1972 *Atomic Structure and Light Scattering in Solids* ed E Burstein (New York: Academic)
[46] Weinstein B A 1976 *Proc. 13th Int. Conf. on Semicond. (Rome)* p 326